Hindawi
Modelling and Simulation in Engineering
Volume 2019, Article ID 3052790, 11 pages
https://doi.org/10.1155/2019/3052790

Research Article

Multiple Slip Effects on MHD Unsteady Flow Heat and Mass Transfer Impinging on Permeable Stretching Sheet with Radiation

Fazle Mabood[1] **and Stanford Shateyi**[2]

[1]*School of Information Technology, Fanshawe College, London, ON, Canada*
[2]*Department of Mathematics, University of Venda, P Bag X5050, Thohoyandou 0950, South Africa*

Correspondence should be addressed to Fazle Mabood; mabood1971@yahoo.com

Received 25 September 2018; Accepted 13 January 2019; Published 12 February 2019

Academic Editor: Michele Calì

This paper reports multiple slip effects on MHD unsteady flow heat and mass transfer over a stretching sheet with Soret effect; suction/injection and thermal radiation are numerically analyzed. We consider a time-dependent applied magnetic field and stretching sheet which moves with nonuniform velocity. Suitable similarity variables are used to transform governing partial differential equations into a system of coupled nonlinear ordinary differential equations. The transformed equations are then solved numerically by applying an implicit finite difference method with quasi-linearization technique. The influences of the various parameters on the velocity temperature and concentration profiles as well as on the skin friction coefficient and Sherwood and Nusselt numbers are discussed by the aid of graphs and tables.

1. Introduction

The Navier–Stokes theory is centered on the central idea of no-slip condition. Many authors have obtained both numerical and analytical solutions by applying no-slip boundary conditions to study velocity and temperature profiles. The importance of slip conditions in microchannel or nanochannels has stimulated much interest on the study of vibrating values [1]. It is now known that a slip can occur if the working fluids contain concentrated suspensions. Soltani and Yilmazor [2] performed using a parallel disk rheometer with emphasis on a wall slip phenomenon on the rheological characterization of highly filled suspensions consisting of a Newtonian matrix, mixed with two different sizes of aluminum power and two different sizes of glass beads. When the fluid is particulates such as suspensions, emulsions foams, and polymer solutions, a partial velocity slip may occur on the stretching boundary. Slip effects can arise in various industrial processes at boundaries of pipes, walls, and/or curved surfaces. A Navier velocity slip condition is a usual approach in studying slip phenomena. Mahanthesh et al. [3] examined three-dimensional flow of nanofluid for the effects of partial slip and chemical reaction towards an exponential stretching sheet. Hayat et al. [4] examined simultaneous effects of slip and heat transfer on peristaltic flow. Motsa and Shateyi [5] studied the problem of a nonlinear boundary value problem arising in rotating disk flow under the effects of a partial slip, thermal diffusion, and diffusion thermo. Shateyi and Mabood [6] have illustrated the impact of slip and viscous dissipation on MHD mixed convection stagnation-point flow over a nonlinear stretching sheet. Khan et al. [7] carried out a study on a two-dimensional flow of an incompressible Williamson fluid of Cattaneo–Christov heat flux type over a linearly stretched surface with the influence of magnetic field, thermal radiation-diffusion, heat generation, and viscous dissipation.

Due to the many applications in engineering and industries, the magnetohydrodynamic fluid flows on a stretching sheet have achieved much importance nowadays [8]. Such applications include the liquid coating on photographic films, the boundary layer through the liquid film in the concentration process, and aerodynamic extrusion of plastic sheets. In addition, a wide range of applications on MHD flow can be found in numerous fields such as electronic cooling, boilers, heat insulation and metal extrusion,

liquid metal fluid oil reservoirs, geothermal systems, nuclear process, micro-MHD pumps, high temperature plasmas, groundwater systems, energy storage units, biological transportation, and thermal energy storage devices . Mabood et al. [9] examined the effects of heat source and chemical reaction on MHD rotating fluid towards a vertical plate influenced by a porous medium. Kumar et al. [10] investigated the impact of frictional heating on MHD ferrofluid with radiation.

Heat transfer, determined by thermal radiation, has vast applications in different technological processes, including missiles, nuclear power plants, satellites and space vehicles, gas turbines, and the numerous propulsion devices for aircraft. Linear radiation is not analytically valid for immense temperature difference. Abbas et al. [11] discussed the effects of radiation in the presence of uniform magnetic field for a nanofluid on a curved stretching surface by incorporating slip effect. Recently, Makinde et al. [12] developed a numerical study of radiation effects on chemically reacting MHD nanofluid influenced by heat source/sink and combined heat and mass transfer analysis for mixed convection flow over vertical surface with radiation and chemical reaction illustrated by Ibrahim et al. [13]. Prasannakumara et al. [14] studied the effects of velocity slip, temperature jump, solutal slip and thermal radiation on a steady flow, heat and mass transfer of an incompressible Jeffrey nanofluid over a horizontal stretching surface. Imtiaz et al. [15] examined unsteady MHD flow of curved stretching surface. Some interesting investigations relevant to flow and heat transfer can be viewed in [16–23].

To the author's knowledge, no studies have this far been communicated with regard to the multiple slips on hydromagnetic unsteady flow and heat and mass transfer influenced by radiation in permeable frame of reference. Numerical solutions are provided for some special cases, while the physical interpretation for the various parameters is discussed with the help of graphs.

2. Governing Equations

A two-dimensional MHD flow of an incompressible electrically conducting fluid over a permeable stretching surface in the presence of thermal radiation is considered. A coordinate system is chosen in such a way that x-axis is measured along the sheet, and y-axis is normal to it as shown in Figure 1. The sheet is moving with nonuniform velocity $U(x,t) = ax/(1-\lambda t)$ along x-axis where a is the stretching rate and λ is the positive constant with the property $\lambda t < 1$. A transverse magnetic field that is assumed to be the function of distance from origin is defined as $B(x) = B_0 x^{-1/2}$ with $B_0 \neq 0$, where x is the coordinate along the surface and B_0 is the magnetic field strength. The induced magnetic field is negligible as compared to the applied magnetic field. Let T_∞ and C_∞ are the free stream temperature and free mass concentration. The governing equations for the continuity, momentum, energy, and concentration can be written:

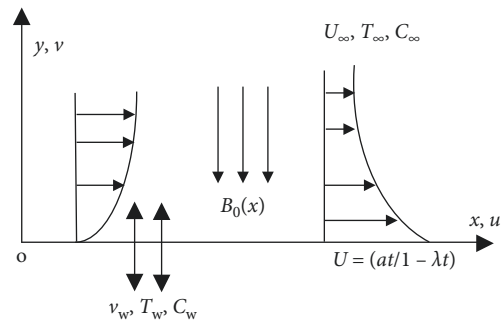

Figure 1: Sketch of the physical model.

$$\frac{\partial u}{\partial x} + \frac{\partial v}{\partial y} = 0, \tag{1}$$

$$\frac{\partial u}{\partial t} + u\frac{\partial u}{\partial x} + v\frac{\partial u}{\partial y} = \nu\frac{\partial^2 u}{\partial y^2} - \frac{\sigma B^2(x)u}{\rho} + g\beta_T(T - T_\infty) + g\beta_C(C - C_\infty), \tag{2}$$

$$\frac{\partial T}{\partial t} + u\frac{\partial T}{\partial x} + v\frac{\partial T}{\partial y} = \alpha\left(1 + \frac{16T_\infty^3\sigma^*}{3k^*\kappa}\right)\frac{\partial^2 T}{\partial y^2}, \tag{3}$$

$$\frac{\partial C}{\partial t} + u\frac{\partial C}{\partial x} + v\frac{\partial C}{\partial y} = D_M\frac{\partial^2 C}{\partial y^2} + D_T\frac{\partial^2 T}{\partial y^2}, \tag{4}$$

where x and y are the coordinates along and normal to the sheet; u and v are the components of the velocity in the x and y directions, respectively; ρ is the density of the fluid; ν is the kinematic viscosity of the fluid; σ is the electrical conductivity; g is the acceleration due to gravity; β_T is the thermal expansion coefficient; β_C is the concentration expansion coefficient; α is the thermal diffusivity; T is the temperature; C is the concentration; D_M is the molecular diffusivity; D_T is the thermal diffusivity; σ^* is the Stefan–Boltzmann constant; and k^* is the mean absorption coefficient.

The boundary conditions for the above described model are:

$$\begin{cases} y = 0 : u = U(x,t) + U_{\text{slip}}, v = v_w, T = T_w(x,t) + T_{\text{slip}}, \\ \quad C = C_w(x,t) + C_{\text{slip}}, \\ y \longrightarrow \infty : u \longrightarrow 0, T \longrightarrow T_\infty, C \longrightarrow C_\infty, \end{cases} \tag{5}$$

where $v_w = v_0/\sqrt{x}$ is the suction/injection velocity.

The temperature of the sheet $T_w(x,t)$ and the concentration $C_w(x,t)$ at the surface are assumed as of the following form:

$$T_w(x,t) = T_\infty + T_0\left(\frac{ax}{2\nu}\right)(1-\lambda t)^{-2},$$
$$C_w(x,t) = C_\infty + C_0\left(\frac{ax}{2\nu}\right)(1-\lambda t)^{-2}, \tag{6}$$

where T_0, and C_0 are the reference temperature and reference concentration, respectively, such that $0 \le T_0 \le T_w$ and $0 \le C_0 \le C_w$. The above expressions are valid if $(1-\lambda t) > 0$.

As per usual, the stream function ψ is defined as $u = \partial\psi/\partial y$ and $v = -\partial\psi/\partial x$ so that equation (1) is satisfied. Let us introduce the following dimensionless functions f, θ, ϕ, and similarity variable η as follows:

$$\begin{cases} \eta = \sqrt{\dfrac{a}{\nu(1-\lambda t)}}\, y, \\ \psi = \sqrt{\dfrac{a\nu}{(1-\lambda t)}}\, x f(\eta), \\ T = T_\infty + T_0\left(\dfrac{ax(1-\lambda t)^{-2}}{2\nu}\right)\theta(\eta), \\ C = C_\infty + C_0\left(\dfrac{ax(1-\lambda t)^{-2}}{2\nu}\right)\phi(\eta). \end{cases} \tag{7}$$

Now substituting equation (7) into equations (2)–(4), we get the following system of nonlinear ordinary differential equations:

$$f''' + ff'' - f'^2 - \delta\left(\frac{\eta}{2}f'' + f'\right) - Mf' + \lambda_1\theta + \lambda_2\phi = 0, \tag{8}$$

$$\frac{1}{\Pr}(1+R)\theta'' + f\theta' - f'\theta - \delta\left(\frac{\eta}{2}\theta' + 2\theta\right) = 0, \tag{9}$$

$$\phi'' + Sc\left(f\phi' - f'\phi\right) - Sc\ \delta\left(\frac{\eta}{2}\phi' + 2\phi\right) + Sc\, S_r\theta'' = 0. \tag{10}$$

The transformed boundary conditions of the problem are

$$\begin{cases} f(0) = f_w, \\ f'(0) = 1 + S_f f''(0), \\ f'(\infty) = 0, \\ \theta(0) = 1 + S_\theta\theta'(0), \\ \theta(\infty) = 0, \\ \phi(0) = 1 + S_\phi\phi'(0), \\ \phi(\infty) = 0, \end{cases} \tag{11}$$

where $\delta = \lambda/a$ is the unsteadiness parameter; $\lambda_1 = g\beta_T T_0/a\nu$ and $\lambda_2 = g\beta_C C_0/a\nu$ are the buoyancy parameters; $\Pr = \nu/\alpha$ is the Prandtl number; $R = 16T_\infty^3\sigma^*/3k^*\kappa$ is the thermal radiation parameter; $M = \sqrt{\sigma/\rho a}B_0$ is the magnetic field parameter; $Sc = \nu/D_M$ is the Schmidt number; $S_r = D_T T_0/\nu C_0$ is the Soret number; and $f_w = -v_w(\sqrt{1-\gamma t}/\sqrt{va})$ is the suction/injection parameter. Here, $f_w = 0$ represents the impermeable surface, $f_w > 0$ represents the suction, and $f_w < 0$ represents the injection of the fluid through permeable surface.

The physical quantities of interest are local skin friction coefficient C_f, local Nusselt number Nu, and local Sherwood number Sh are defined as

$$C_f = \frac{\mu}{\rho U_w^2}\left(\frac{\partial u}{\partial y}\right)_{y=0}, \tag{12}$$

$$\mathrm{Nu} = \frac{x}{\kappa(T_w - T_\infty)}\left[\kappa\left(\frac{\partial T}{\partial y}\right)_{y=0} - \frac{4\sigma^*}{3k^*}\left(\frac{\partial T^4}{\partial y}\right)_{y=0}\right], \tag{13}$$

$$\mathrm{Sh} = -\frac{x}{(C_w - C_\infty)}\left(\frac{\partial C}{\partial y}\right)_{y=0}. \tag{14}$$

Substitute equation (7) into equations (12)–(14) to obtain the final dimensionless form:

$$\begin{cases} \mathrm{Cfr} = \sqrt{\mathrm{Re}_x}\, C_f = f''(0), \\ \mathrm{Nur} = \dfrac{\mathrm{Nu}}{\sqrt{\mathrm{Re}_x}} = -(1+R)\theta'(0), \\ \mathrm{Shr} = \dfrac{\mathrm{Sh}}{\sqrt{\mathrm{Re}_x}} = -\phi'(0), \end{cases} \tag{15}$$

where $\mathrm{Re}_x = U_w x/\nu$ is the local Reynolds number, Cfr is the reduced skin friction, Nur is the reduced Nusselt number, and Shr is the reduced Sherwood number.

3. Numerical Method

The reduced ordinary differential equations (9)–(11) subject to the boundary conditions (12) were solved numerically using an implicit finite difference method with quasi-linearization technique. The details of the proposed method can be found in the studies of Mabood et al. [21], Inoyue and Tate [22], and Bellman and Kalaba [23]. The effects of the various parameters on the velocity, temperature, concentration, and heat and mass transfer rates are investigated. The step size and convergence criteria were taken as $\Delta\eta = 0.001$ and 10^{-6}, respectively. The asymptotic boundary conditions in equation (12) were approximated by using a value of 10 for the similarity variable $\eta_{\max}$ as follows:

$$\begin{aligned} \eta_{\max} &= 10, \\ f'(10) = \theta(10) &= \phi(10) = 0. \end{aligned} \tag{16}$$

The choice of $\eta_{\max} = 10$ ensures that all numerical solutions approached the asymptotic values correctly.

4. Results and Discussion

In order to validate our current results and to determine the accuracy of the present analysis, comparisons with available results of the skin friction coefficient $-f''(0)$ for the unsteady flow of viscous incompressible Newtonian fluid are done. In Table 1, we compare our results of the skin friction coefficient generated by Chamkha et al. [16]. In this table, we observe that there is an excellent agreement between our results, and those observe in this table that the skin friction coefficient increases with the increasing values of the stretching parameter. In Table 2, we observe that there is an excellent agreement between our

Table 1: Comparison of $-f''(0)$ for various values of δ when $f_w = M = \lambda_1 = \lambda_2 = S_f = 0$.

δ	Chamkha et al. [16]	Present
0.8	1.261512	1.261042
1.2	1.378052	1.377724

Table 2: Comparison of $-f''(0)$ for various values of M when $f_w = \delta = S_f = 0$.

M	Mabood and Das [8]	Present
0	−1.000008	−1.0000084
1	1.4142135	1.41421356
5	2.4494897	2.44948974
10	3.3166247	3.31662479
50	7.1414284	7.14142843
100	10.049875	10.0498756
500	22.383029	22.3830293
1000	31.638584	31.6385840

present results with those previously obtained by Mabood and Das [8]. We also observe in this table that, as the magnetic parameter M increases, the skin friction significantly increases due to the Lorentz drag force caused by electromagnetism increases. Lastly, Table 3 depicts the comparison of our present results to those obtained by Ali [17] when investigating the effect of the Prandtl number on the heat transfer rate. We observe that the heat transfer rate on the surface is greatly affected by the Prandtl number. Increasing the Prandtl number increases the rate of heat transfer on the stretching surface.

Figure 2 depicts the effect of increasing the magnetic field parameter M on the velocity profiles with (Figure 2(b)) and without (Figure 2(a)) hydrodynamic slip. We observe in both cases that the velocity profiles are reduced with increasing values of the magnetic parameter. Physically, the presence of the transverse magnetic field in the fluid flow produces a drag-like force called the Lorentz which in turn decelerates the fluid motion. However, the existence of the hydrodynamic slip as can be clearly seen in Figure 2 increases the velocity boundary layer. We also observe in Figure 2 that suction reduces the velocity boundary layer. Thus, suction can be used as a stabilizing mechanism to delay the transition from the laminar boundary layer flow to turbulent flow.

The effect of varying the thermal buoyancy parameter on the velocity distribution is depicted in Figure 3 and that of solutal buoyancy parameter is shown in Figure 4. Increasing values of the buoyancy parameters leads to the increase in the temperature and solutal gradients. Physically, this explains why the velocity profiles increase as more forces are added with these increases in buoyancy parameters δ. We also observe in Figure 3 that the velocity profiles decrease as the unsteadiness parameter increases. Also increasing the values of thermal radiation parameter R causes the profiles of the velocity to increase (Figure 4).

The influence of the magnetic parameter M and thermal radiation R on the temperature profiles is shown on Figure 5. Reduction of the flow velocity due to the increase of the magnetic field strength causes the temperature profiles (Figure 5) and concentration profiles (Figure 6) to increase. Physically, applying the magnetic field heats up the fluid and thus reduces the heat and mass transfer rates from the wall causing increases in fluid temperature and concentration distributions. We also observe in Figure 5 that the fluid temperature increases with increasing values of the thermal radiation parameter R. The effect of radiation in the thermal boundary layer (equation (3)) is equivalent with an increased thermal diffusivity.

Table 3: Comparison of heat transfer rate $-\theta'(0)$ when $M = f_w = S_f = S_\theta = \delta = \lambda_1 = \lambda_2 = R_d = 0$.

Pr	Ali [17]	Present
0.72	0.8058	0.8088
1	0.9691	1.0000
3	1.9144	1.9237
10	3.7006	3.7207

Figure 7 depicts the influence of thermal buoyancy parameter on the dimensionless temperature profiles. It is clearly observed that an increase in the thermal Grashof number causes a decrease in the thermal boundary layer thickness and consequently the fluid temperature decreases due to the buoyancy effect. We also observe in Figure 7 that the temperature profiles are lower for suction $f_w > 0$. Figure 8 shows the effect of the stretching parameter δ and the Prandtl number on the temperature distribution. We observe in this figure that the temperature profiles are reduced with increasing values of the Prandtl number. It is also observed in this figure that the temperature profiles are reduced with increasing values of the stretching parameter. Figure 6 displays the effect of varying the Schmidt number and the magnetic field parameter on the concentration profiles. The Schmidt number represents the relative ease of the molecular momentum and mass transfer, and it is very important in multiphase flows. The effect of increasing values of the Schmidt number is to reduce the momentum boundary layer, and this leads to the thinning of the diffusion layer.

Figure 9 depicts the effects of magnetic, unsteadiness, slip velocity, and suction/injection parameters on the skin friction coefficient. We observe in this figure that $|f''(0)|$ decreases with increasing values of the slip velocity S_f and buoyancy parameters. But it increases with increasing values of the magnetic and suction parameters. Figure 10 exhibits the nature of the heat transfer coefficient with the thermal radiation, thermal slips, buoyancy, magnetic, and suction and injection parameters. We observe in this figure that increasing the magnetic field strength M strongly suppresses the Nusselt numbers. Physically, an extra work done by dragging the fluid against the action of transverse magnetic field is then dissipated on heat energy in the boundary layer. This leads to the heating up of the boundary layer resulting in more heat transferred to the fluid flow. Thus heat transfer to the wall is reduced. The rate of heat transfer on the stretching surface is significantly enhanced by the increasing values of the thermal radiation parameter, suction parameter, and solutal buoyancy parameter. But opposite

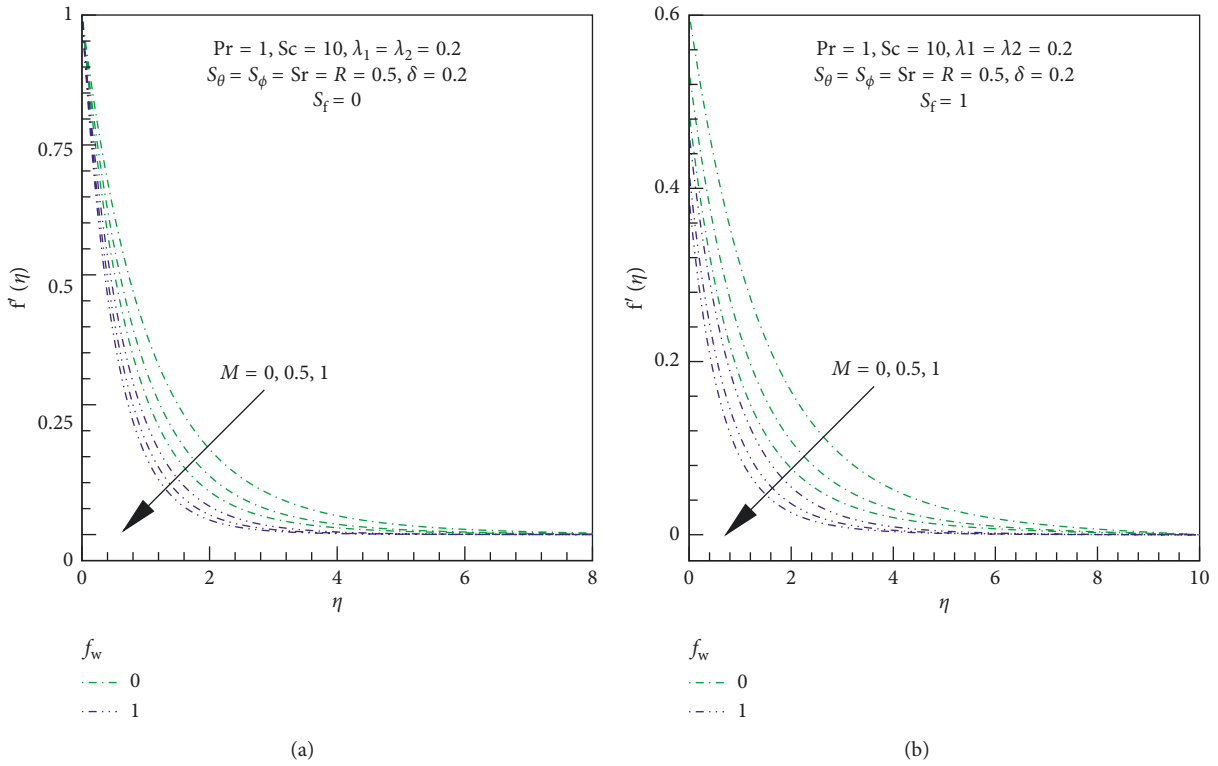

Figure 2: Effects of M and f_w on dimensionless velocity. (a) No hydrodynamic slip. (b) With hydrodynamic slip.

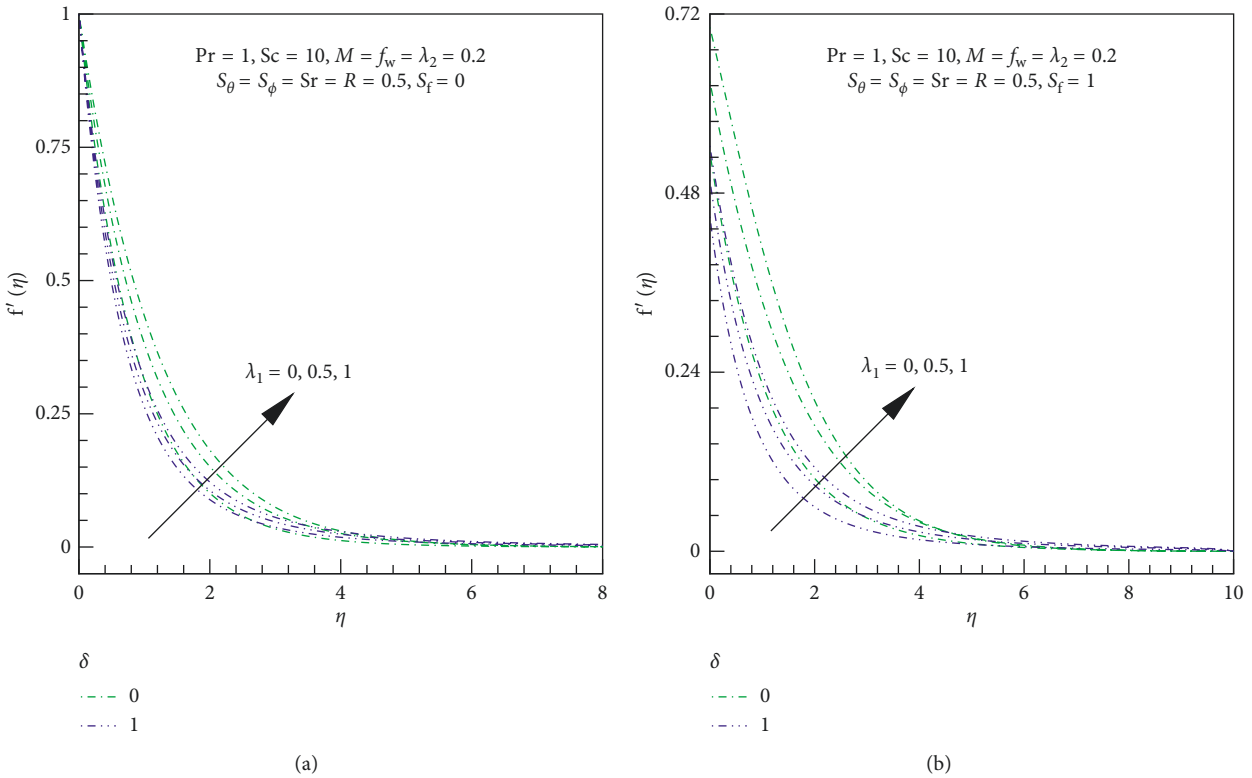

Figure 3: Effects of λ_1 and δ on dimensionless velocity. (a) No hydrodynamic slip. (b) With hydrodynamic slip.

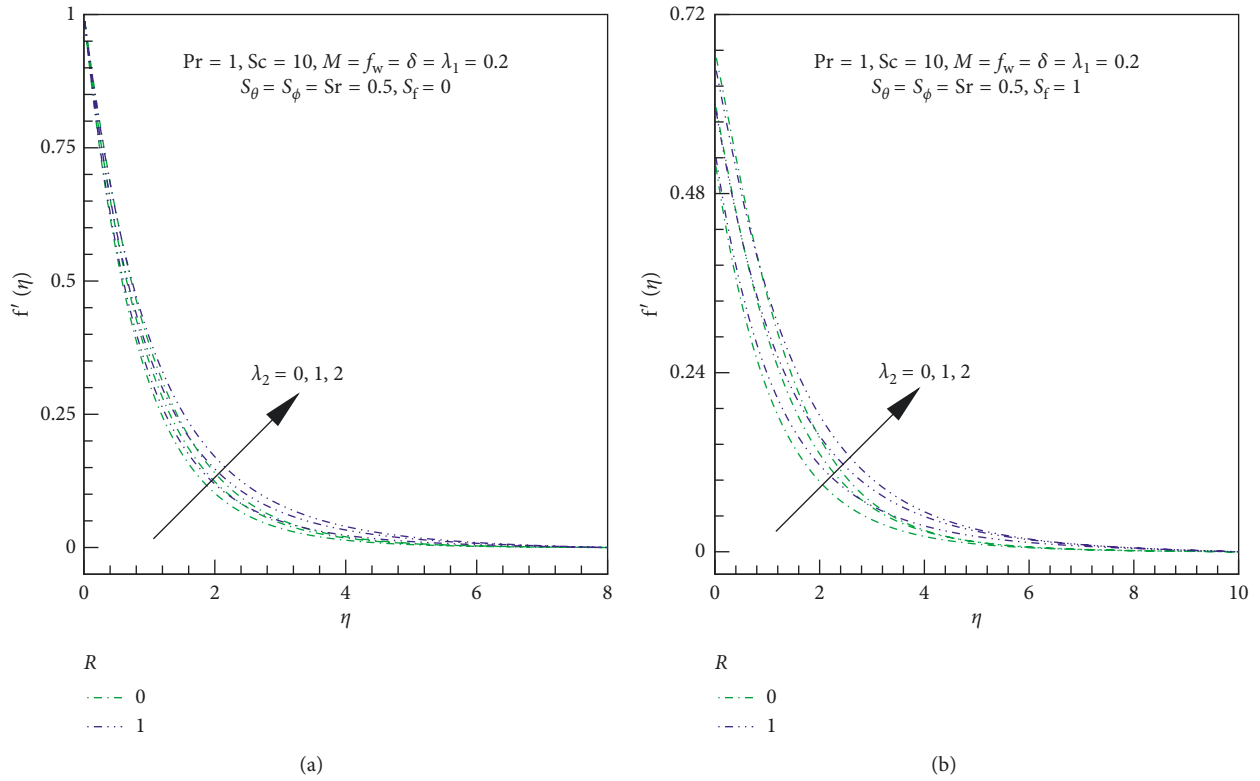

Figure 4: Effects of λ_2 and R on dimensionless velocity. (a) No hydrodynamic slip. (b) With hydrodynamic slip.

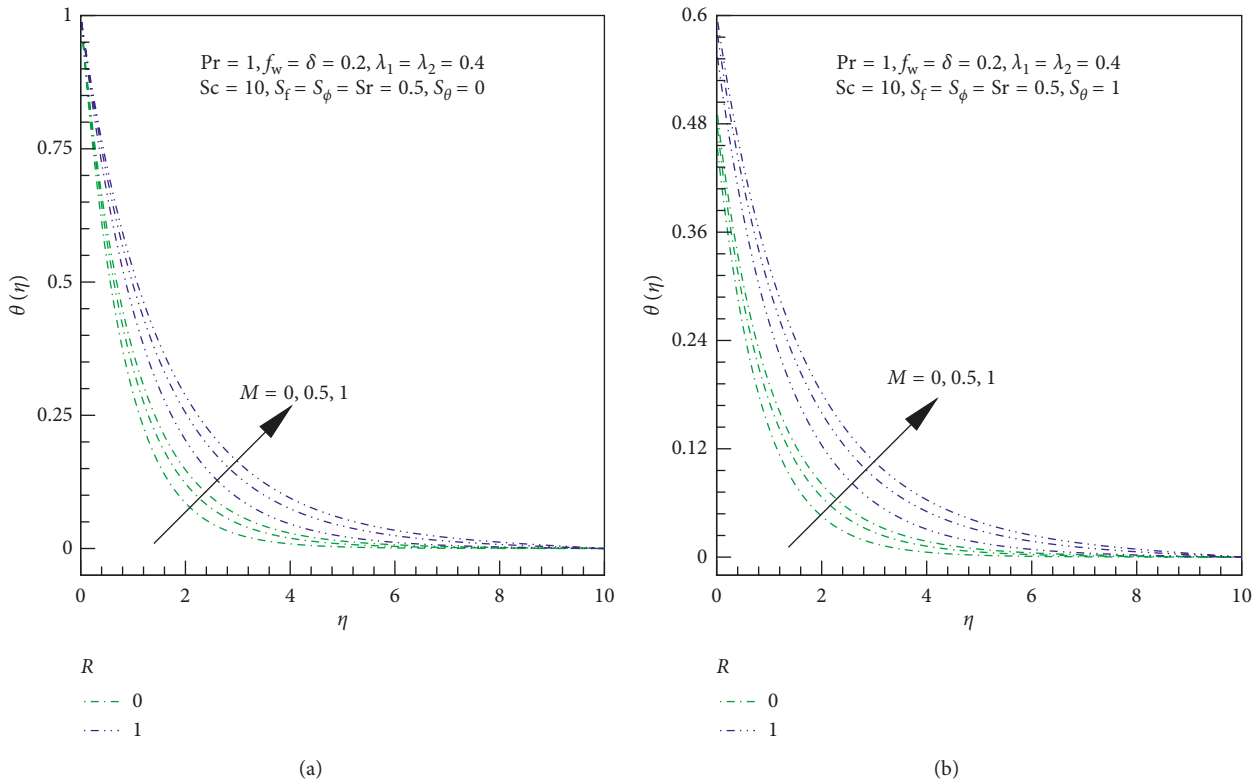

Figure 5: Effects of M and R on dimensionless temperature. (a) No thermal slip. (b) With thermal slip.

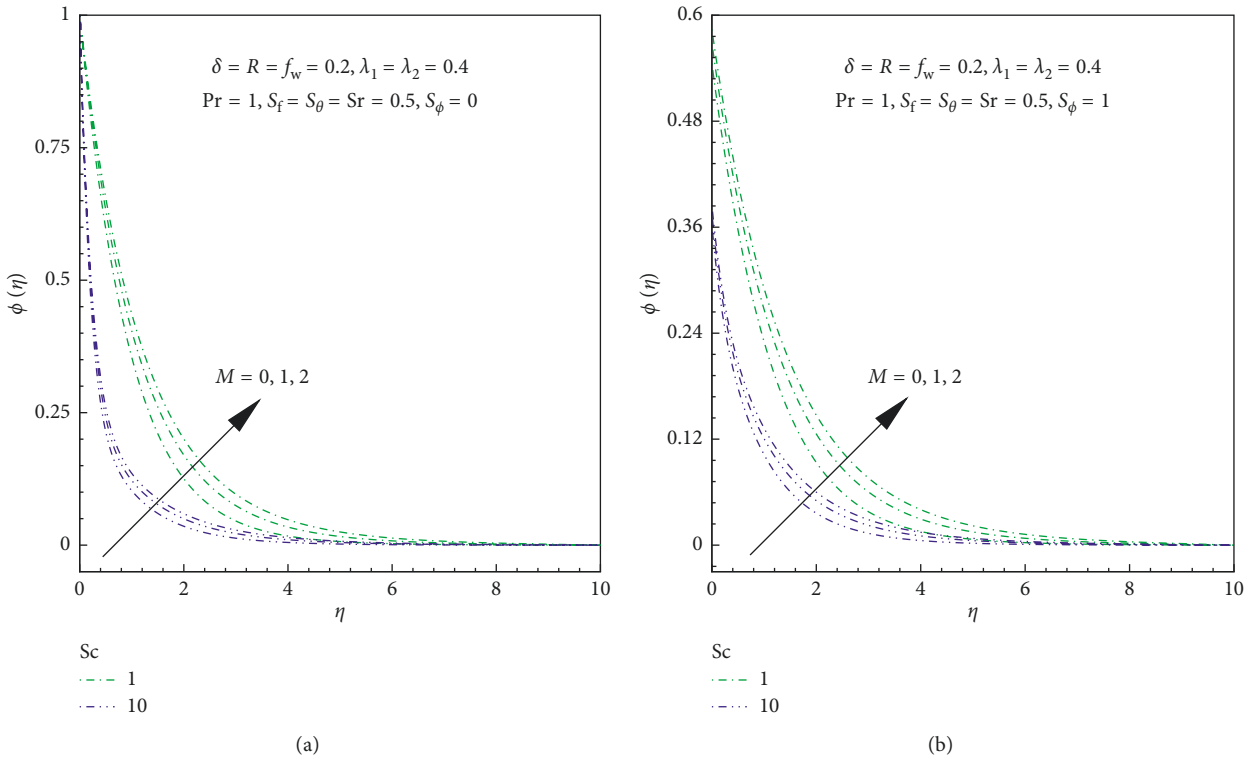

Figure 6: Effects of M and Sc on dimensionless concentration. (a) No thermal slip. (b) With thermal slip.

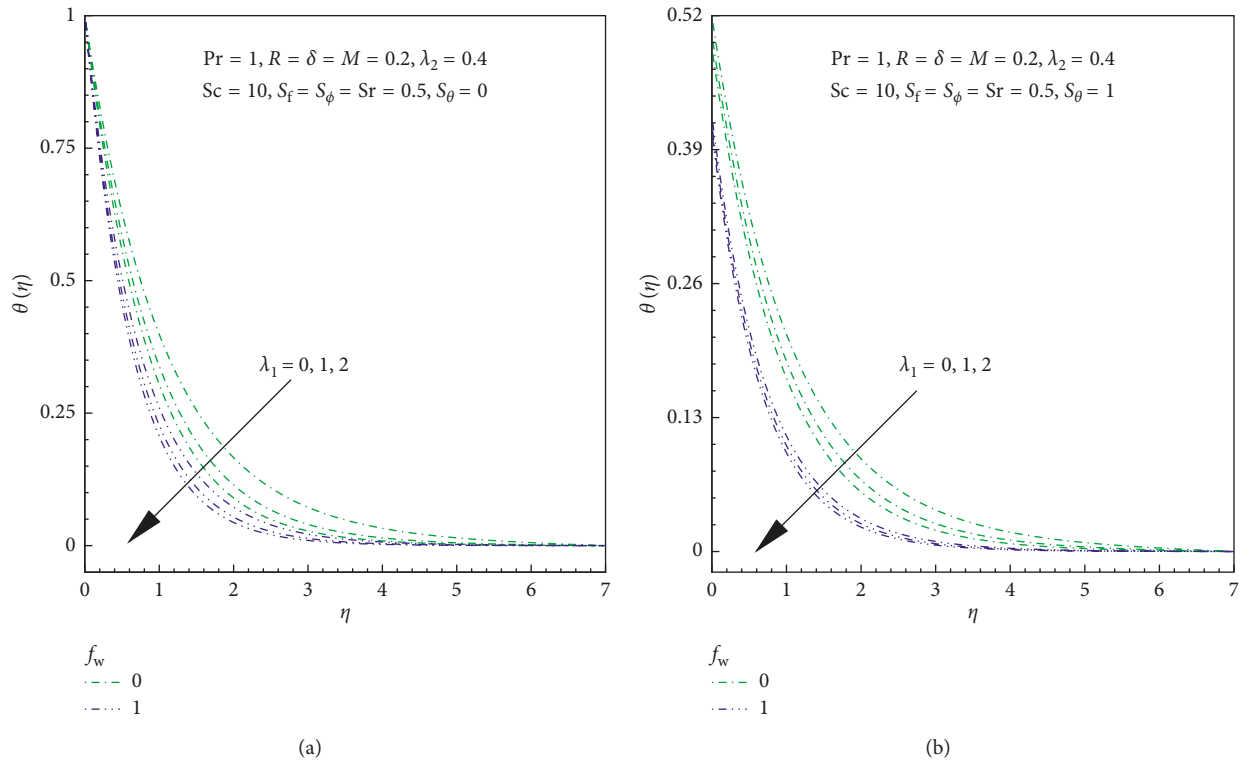

Figure 7: Effects of λ_1 and f_w on dimensionless temperature. (a) No thermal slip. (b) With thermal slip.

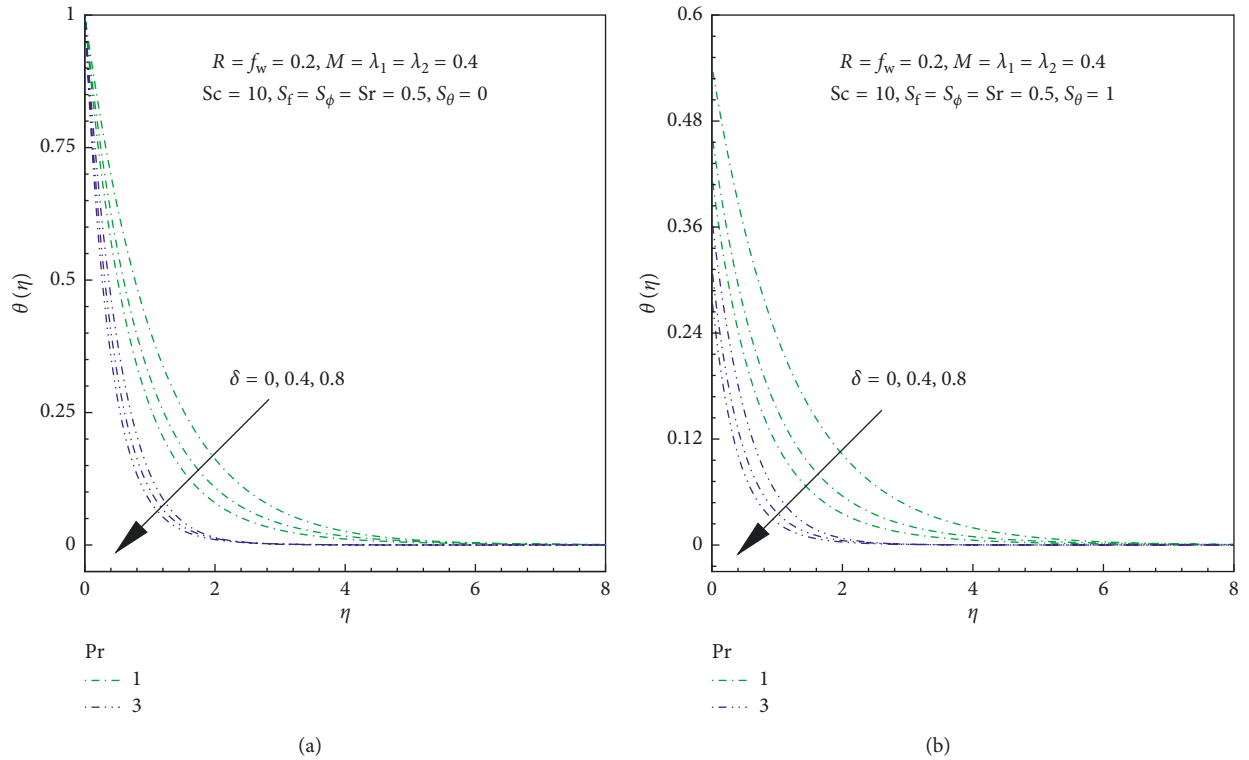

Figure 8: Effects of δ and Pr on dimensionless temperature. (a) No thermal slip. (b) With thermal slip.

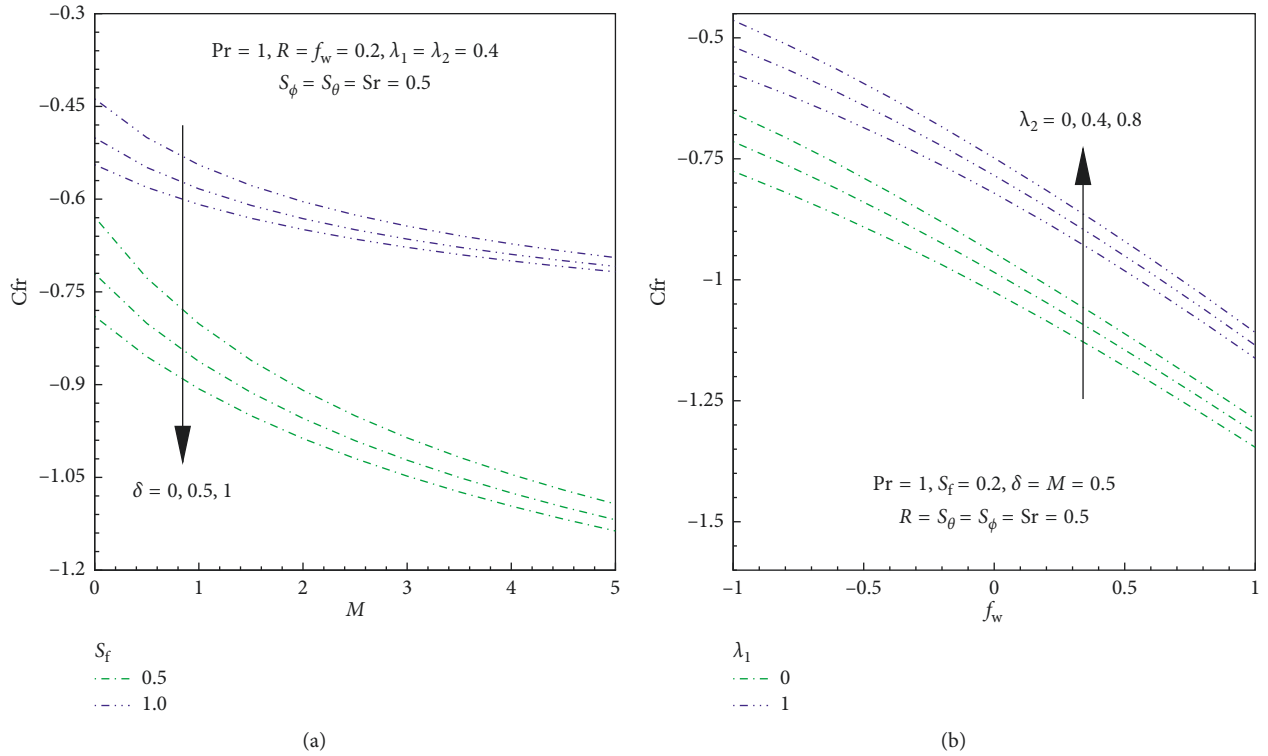

Figure 9: Effects of $M, \delta, S_f, \lambda_1, \lambda_2$, and f_w on the skin friction coefficient.

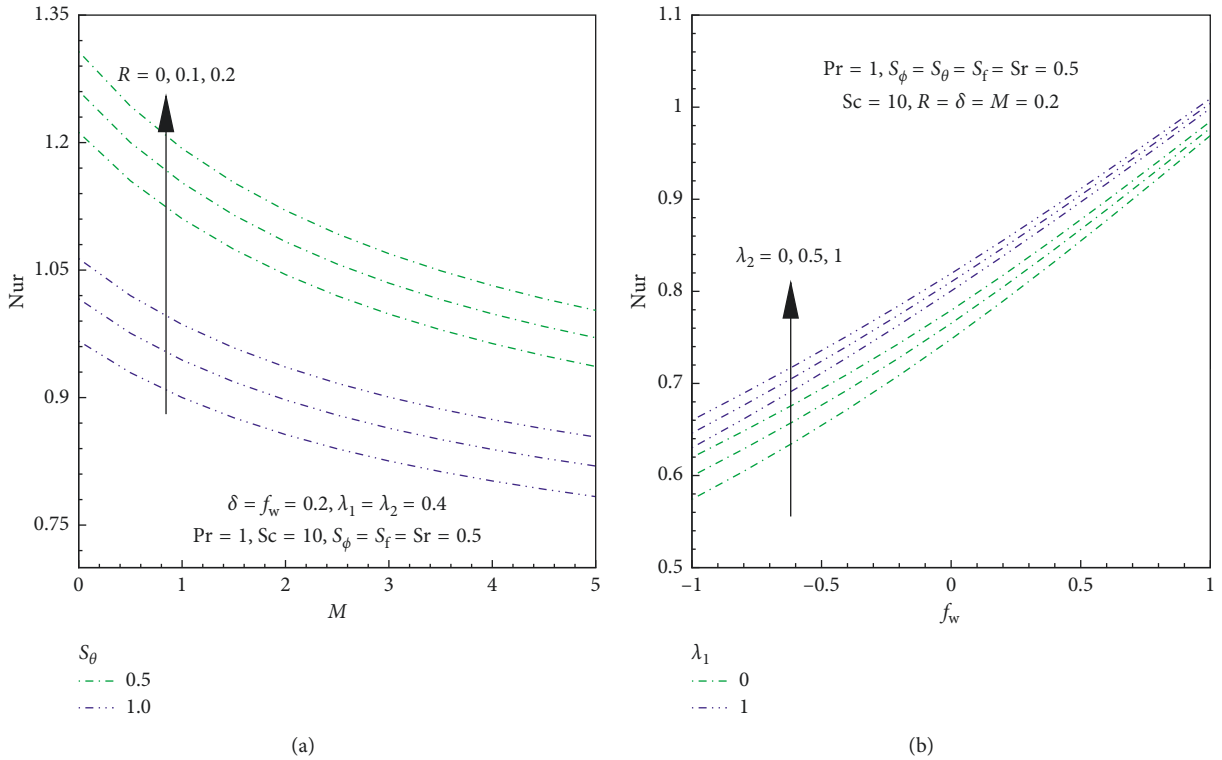

FIGURE 10: Effects of $M, R, S_\theta, \lambda_1, \lambda_2$, and f_w on the reduced Nusselt number.

responses are observed with increasing values of thermal buoyancy and injection parameters.

Finally, Figures 11(a) and 11(b) present the Sherwood distributions with variation of the Schmidt number, magnetic parameter, solutal slip parameter, Soret number, sectional injection, and unsteadiness parameter. We observe in these figures that the mass transfer rate decreases with magnetic and solutal slip parameters. We can clearly see in these figures that the rate of mass transfer increases with the Schmidt number and reduces the solutal boundary layer thickness. Finally, we observe that the Sherwood number is significantly elevated with increasing values of the unsteadiness parameter.

5. Conclusions

In this article, a mathematical model has been developed to simulate an unsteady two-dimensional magnetohydrodynamic flow of an incompressible electrically conducting fluid over a permeable stretching surface in the presence of multiple slip effects, Soret effect, and thermal radiation. Suitable similarity variables have been used to transform the boundary layer conservation equations into a nondimensional, coupled, and nonlinear system of ordinary differential equations. The resultant system of ordinary differential equations was then numerically solved using an implicit finite difference method with quasi-linearization technique. We also used special cases of the present model to verify our results with previous studies. A parametric study was performed to explore the effects of various governing parameters on the flow and heat and mass transfer characteristics. The following conclusions can be drawn from the present study:

(i) Increasing the values of the magnetic field parameter, suction parameter, slip parameters, and unsteady parameter leads to the deceleration of the fluid velocity near the boundary layer region.

(ii) The velocity profiles are increased with increasing values of the injection parameter, buoyancy parameters, and thermal radiation.

(iii) The velocity profiles are found to be reduced with increasing values of the magnetic parameter, suction parameter, and slip velocity parameter.

(iv) Increments in thermal radiation, magnetic field parameter, and slip parameters yield enhancement in the fluid temperature. This in turn leads to rapid reductions in the heat transfer rate. However, the opposite effect is experienced with increasing values of thermal buoyancy parameter, Prandtl number, and unsteadiness parameter.

(v) The skin friction coefficient increases with the increase of the magnetic field, Prandtl and Schmidt numbers, unsteadiness parameter, and suction parameter, but the effect is opposite for increasing values of slip parameters and buoyancy parameters.

(vi) The concentration profiles are enhanced by increasing values of the magnetic field but are reduced by increasing values of the Schmidt number and buoyancy and slip parameters.

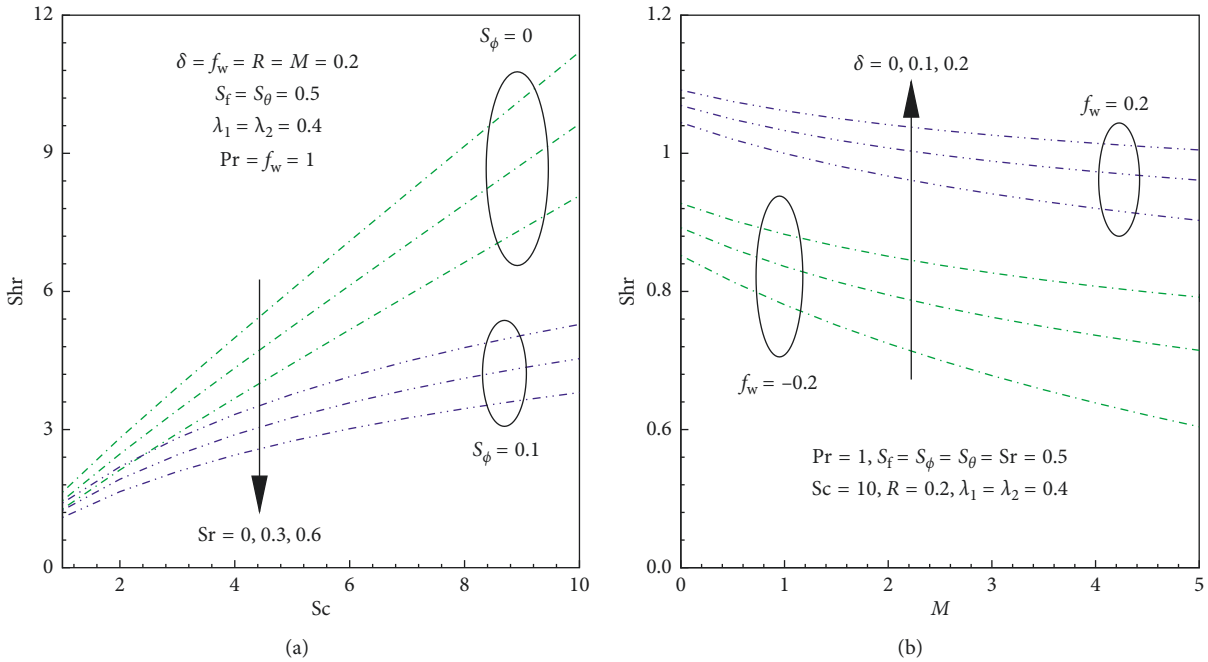

Figure 11: Effects of $Sc, Sr, S_\phi, \delta, M$, and f_w on the reduced Sherwood number.

Nomenclature

a: Stretching rate
B_o: Magnetic field of constant strength
C_f: Local skin friction coefficient
c_p: Specific heat
C: Concentration of the fluid
C_w: Stretching sheet concentration
C_0: Reference concentration
C_∞: Ambient concentration
Cfr: Reduced skin friction
D_M: Molecular diffusivity
D_T: Thermal diffusivity
f_w: Suction/injection parameter
k^*: Mean absorption coefficient
M: Magnetic parameter
Nur: Reduced Nusselt number
Pr: Generalized Prandtl number
Re_x: Local Reynolds number
Shr: Reduced Sherwood number
Sc: Schmidt number
S_r: Soret number
S_f: Velocity slip
S_θ: Thermal slip
S_ϕ: Solutal slip
T: Temperature of the fluid
T_w: Stretching sheet temperature
T_0: Reference temperature
T_∞: Ambient temperature
u: Velocity along the x direction
v: Velocity along the y direction
x, y: Coordinates
$\theta(\eta), \phi(\eta)$: Nondimensional temperature and concentration parameter
η: Similarity variable
υ: Kinematic viscosity
α: Thermal diffusivity
β_T: Thermal expansion coefficient
β_C: Concentration expansion coefficient
τ: Stress tensor
δ: Unsteadiness parameter
λ: Constant
ρ: Density of the fluid
λ_1: Thermal buoyancy parameter
λ_2: Solutal buoyancy parameter
σ^*: Stefan–Boltzmann constant.

Data Availability

No data used in this manuscript.

Conflicts of Interest

The authors declare that there are no conflicts of interest regarding the publication of this paper.

References

[1] C. Derek, D. C. Tretheway, and C. D. Meinhart, "Apparent fluid slip at hydrophobic microchannel walls," *Physics of Fluids*, vol. 14, no. 3, pp. 9–12, 2002.

[2] F. Soltani and l. Yilmazer, "Slip velocity and slip layer thickness in flow of concentrated suspensions," *Journal of Applied Polymer Science*, vol. 70, no. 3, pp. 515–522, 1998.

[3] B. Mahanthesh, F. Mabood, B. J. Gireesha, and R. S. R. Gorla, "Effects of chemical reaction and partial slip on the three dimensional flow of a nanofluid impinging on an exponentially stretching surface," *European Physical Journal Plus*, vol. 132, no. 3, 2017.

[4] T. Hayat, S. Hina, and N. Ali, "Simultaneous effects of slip and heat transfer on the peristaltic flow," *Communications in Nonlinear Science and Numerical Simulation*, vol. 15, no. 6, pp. 1526–1537, 2010.

[5] S. S. Motsa and S. Shateyi, "Successive linearization analysis of the effects of partial slip, thermal diffusion, and diffusion-thermo on steady MHD convective flow due to a rotating disk," *Mathematical Problems in Engineering*, vol. 2012, Article ID 397637, 15 pages, 2012.

[6] S. Shateyi and F. Mabood, "MHD mixed convection slip flow near a stagnation-point on a non-linearly vertical stretching sheet in the presence of viscous dissipation," *Thermal Science*, vol. 21, no. 6, pp. 2731–2745, 2017.

[7] M. D. S. Khan, M. D. M. Rahman, S. M. Arifuzzamanc, P. Biswas, and I. Karim, "Williamson fluid flow behaviour of MHD convective-radiative Cattaneo–Christov heat flux type over a linearly stretched-surface with heat generation and thermal-diffusion," *Frontiers in Heat and Mass Transfer (FHMT)*, vol. 9, p. 15, 2017.

[8] F. Mabood and K. Das, "Melting heat transfer on hydromagnetic flow of a nanofluid over a stretching sheet with radiation and second-order slip," *The European Physical Journal Plus*, vol. 131, no. 1, p. 3, 2016.

[9] F. Mabood, S. M. Ibrahim, and G. Lorenzini, "Chemical reaction effects on MHD rotating fluid over a vertical plate embedded in porous medium with heat source," *Journal of Engineering Thermophysics*, vol. 26, no. 3, pp. 399–415, 2017.

[10] K. A. Kumar, J. V. Ramana Reddy, V. Sugunamma, and N. Sandeep, "Impact of frictional heating on MHD radiative ferrofluid past a convective shrinking surface," *Defect and Diffusion Forum*, vol. 378, pp. 157–174, 2017.

[11] Z. Abbas, Y. Wang, T. Hayat, and M. Oberlack, Slip effects and heat transfer analysis in a viscous fluid over an oscillatory stretching surface," *International Journal for Numerical Methods in Fluids*, vol. 59, no. 4, pp. 443–458, 2009.

[12] O. Makinde, F. Mabood, and M. Ibrahim, "Chemically reacting on MHD boundary-layer flow of nanofluids over a non-linear stretching sheet with heat source/sink and thermal radiation," *Thermal Science*, vol. 22, no. 1, pp. 495–506, 2018.

[13] S. M. Ibrahim, P. V. Kumar, G. Lorenzini, E. Lorenzini, and F. Mabood, "Numerical study of the onset of chemical reaction and heat source on dissipative MHD stagnation point flow of casson nanofluid over a nonlinear stretching sheet with velocity slip and convective boundary conditions," *Journal of Engineering Thermophysics*, vol. 26, no. 2, pp. 256–271, 2017.

[14] B. C. Prasannakumara, M. R. Krishnamurthy, B. J. Gireesha, and R. S. R. Gorla, "Effect of multiple slips and thermal radiation on MHD flow of jeffery nanofluid with heat transfer," *Journal of Nanofluids*, vol. 5, no. 1, pp. 82–93, 2016.

[15] M. Imtiaz, T. Hayat, A. Alsaedi, and A. Hobiny, "Homogeneous-heterogeneous reactions in MHD flow due to an unsteady curved stretching surface," *Journal of Molecular Liquids*, vol. 221, pp. 245–253, 2016.

[16] A. J. Chamkha, A. M. Aly, and M. A. Mansour, "Similarity solution for unsteady heat and mass transfer from a stretching surface embedded in a porous medium with suction/injection and chemical reaction effects," *Chemical Engineering Communications*, vol. 197, no. 6, pp. 846–858, 2010.

[17] M. E. Ali, "Heat transfer characteristics of a continuous stretching surface," *Wärme-und Stoffübertragung*, vol. 29, no. 4, pp. 227–234, 1994.

[18] S. M. Ibrahim, F. Mabood, P. V. Kumar, G. Lorenzini, and E. Lorenzini, "Cattaneo-Christov heat flux on UCM flow across a melting surface with cross diffusion and double stratification," *Italian Journal of Engineering ScienceTecnica Italiana*, vol. 62, no. 1, pp. 7–16, 2018.

[19] S. Shateyi, F. Mabood, and G. Lorenzini, "Casson fluid flowfree convective heat and mass transfer over an unsteady permeable stretching surface considering viscous dissipation," *Journal of Engineering Thermophysics*, vol. 26, no. 1, pp. 39–52, 2017.

[20] F. Mabood, A. Shafiq, T. Hayat, and S. Abelman, "Radiation effects on stagnation point flow with melting heat transfer and second order slip," *Results in Physics*, vol. 7, pp. 31–42, 2017.

[21] F. Mabood, S. Ibrahim, G. Lorenzini, and E. Lorenzin, "Radiation effects on Williamson nanofluid flow over a heated surface with magnetohydrodynamics," *International Journal of Heat and Technology*, vol. 35, no. 1, pp. 196–204, 2017.

[22] K. Inoyue and A. Tate, "Finite difference version of quasilinearization applied to boundary layer equations," *AIAA Journal*, vol. 12, no. 4, pp. 558–560, 1974.

[23] R. E. Bellman and R. E. Kalaba, *Quasilinearization and Non-Linear Boundary Value Problems*, America Elsevier Publishing Co. Inc., New York, NY, USA, 1965.